Numerical Study of an AMTEX '75 Oceanic Cyclone[1]

TSING-CHANG CHEN
Department of Earth Sciences, Iowa State University, Ames, 50011

CHIA-BO CHANG[2] AND DONALD J. PERKEY
Department of Physics and Atmospheric Science, Drexel University, Philadelphia, PA 19104

(Manuscript received 14 July 1982, in final form 14 June 1983)

ABSTRACT

The diabatic effects of latent heat release, boundary layer moisture and heat flux from the ocean surface, and large-scale forcing due to upper-level systems are three physical processes affecting oceanic cyclogenesis. Detailed analyses of a major winter storm which occurred during the initial phase of the Air Mass Transformation Experiment in 1975 (AMTEX '75) indicated that the role of these three processes was vital to the cyclone's development. To gain further insight into their influence, a control and three numerical experiments were performed using a multi-level moist primitive equation model with fine vertical resolution in the boundary layer.

The simulation which included complete physics faithfully reproduced the major features of the observed system. It was found that latent heating had a profound impact on the middle-level baroclinicity, the intensity and phase speed of the storm, and the vertical coupling within the simulated system. Without the surface moisture and heat source, the effects of the model moist processes were greatly reduced, suggesting that the effects of air–sea interaction are important even for short-range (24 h) numerical weather prediction of oceanic cyclones. The exclusion of the large-scale forcing resulted in a rather shallow model system. The dynamic response to diabatic heating became disorganized without the large-scale influence.

1. Introduction

The Air Mass Transportation Experiment (AMTEX) was designed to investigate the exchange of energy and momentum between the sea and atmosphere, and the impact of these exchange processes on the generation and development of meteorological disturbances on a variety of scales. One such disturbance is a low-level (surface to 700 mb) subsynoptic-scale (diameter of the order of 1000 km) cyclone. Some of these low-level cyclones develop into extratropical cyclones while others decay within 24–48 h.

A disturbance of the developing type was initiated over the ocean east of Taiwan at the beginning of AMTEX '75. This disturbance moved northeastward along the axis of the Kuroshio Current and merged with an upper-level large-scale trough system. Within 24 h an intense extratropical oceanic cyclone developed. Because the study of oceanic cyclones has long been hindered by the lack of observations, the AMTEX field observations of this cyclone provide a unique opportunity to examine oceanic cyclogenesis.

Saito (1977) analyzed the development of this AMTEX cyclone using a spatial smoothing scheme which separated the subsynoptic-scale and synoptic-scale components. He concluded qualitatively that the primary factor responsible for the development of this cyclonic system was the deepening of the large-scale trough. Chen and Chang (1982) reanalyzed the genesis and development of this system using the data compiled by the AMTEX group at the University of Oklahoma (Soliz and Fein, 1980). They suggested that in addition to the large-scale trough (i.e., large-scale forcing), latent heat release and sensible heat and moisture fluxes from the ocean surface may have had a profound effect on the initiation and development of the storm.

AMTEX was concluded seven years ago and the scientific results of numerous studies regarding AMTEX were summarized in GARP Publications Series No. 24 (1981). However, the report pointed out that there were few numerical simulation results from which to gain insight into the genesis processes of oceanic disturbances. The purpose of this study is to examine the relative roles of latent heat release, air–sea interaction and large-scale forcing in oceanic cyclogenesis using a fine-mesh numerical model.

The model structure and the numerical experiments designed to evaluate the relative roles of these processes in the cyclone's development are discussed in Sections 2 and 3, respectively. The synoptic structure of the cyclone is described in Section 4. Verification of the

[1] Part of this study was presented at the Fifth Numerical Weather Prediction Conference of the American Meteorological Society, Monterey, November 1981.

[2] Visiting Research Associate, Department of Earth Sciences, Iowa State University, Spring 1981.

model simulations are discussed in Section 5, while Section 6 presents comparisons of three experiments with the control experiment.

2. Model description

Drexel University's Limited Area Mesoscale Prediction System (LAMPS) was used to perform the numerical experiments in this study. The model equations and physics are summarized in the Appendix. A brief discussion is given here of the most relevant model features for the purposes of this investigation.

Since most of the area of interest is over the ocean, terrain effects are not important. Thus for these investigations the model was framed in a constant height vertical coordinate. The model levels were 0.0, 0.025, 0.375, 0.75, 1.25, 2.0, 3.0, 4.5, 6.0, 7.5, 9.0, 10.5, 12.0, 14.0 and 16.0 km. Note that the fine vertical resolution in the lower layer is an important model feature for a numerical study of the impact of the air–sea interaction on a low-level cyclone. Fully moist physics (Perkey, 1976) and an active cumulus parameterization scheme (Kreitzberg and Perkey, 1976, 1977) as employed by the system are necessary for testing the effects of latent heat. The ability to use either near-constant lateral boundaries (porous sponge) or time-dependent boundaries as described by Perkey and Kreitzberg (1976) is advantageous for isolating the effects of the large-scale forcing (see discussion in Section 3).

The LAMPS model was modified such that a bulk-aerodynamics formulation was used to treat the sensible heat (F_θ) and moisture (F_q) fluxes from the sea surface. These formulations are

$$F_\theta = \rho C_D |V|_0 (T_w - T_0),$$

$$F_q = \rho C_D |V|_0 (q_w - q_0).$$

The subscripts w and 0 refer to the sea surface and the lowest model level, respectively. The drag coefficient C_D used in this study was 2×10^{-3}. V_0 and ρ are the magnitude of surface wind and surface air density.

3. Design of the numerical experiments

The numerical experiments were designed to investigate the influence of latent heat release, sensible heat and moisture flux from the ocean, and large-scale forcing on the development of the AMTEX disturbance. The control and three 24 h simulation experiments are described as follows:

1) The control experiment included the complete LAMPS moist physics and time-dependent boundary conditions at the lateral boundaries. This experiment is referred to as the Control.

2) Experiment 1 was similar to the Control, but without latent heat release. This experiment is referred to as E1.

3) Experiment 2 (E2) was similar to the Control, but without sensible heat and moisture fluxes from the sea surface.

4) Experiment 3 (E3) was similar to the Control except that porous sponge lateral boundary conditions, instead of time-dependent conditions, were applied.

The results of the Control were compared with observations to verify the performance of the model and with results of the other three experiments to determine the relative roles of the three tested processes. Elimination of the moisture and thus the latent heat release in E1 is designed to quantify the effect of latent heat release on the development of the cyclone's structure.

E2 is designed to determine whether, during a 24 h period, sensible heat and moisture fluxes from the sea surface can have a significant impact on oceanic cyclogenesis as suggested by Agee and Howley (1977) and Kung and Siegel (1979). It is believed that the supply of sensible and latent heat from the warm sea surface may be one of the major causes inducing air mass modification and the development of low-level weather disturbances. In fact, calculations by Sheu and Agee (1977) using AMTEX '75 data have shown that the total heat flux from the sea to the atmosphere may achieve values as large as 1200 W m^{-2}.

The application of porous sponge lateral boundary conditions in E3 instead of time-dependent boundary conditions is designed to eliminate the eastward propagation of the large-scale trough into the model domain through the domain's western boundary. Therefore, the coupling of the low-level cyclone and the upper level large-scale system is suppressed.

The model was initialized for all experiments at 1200 GMT 13 February 1975. The initial state was interpolated from gridded data which were objectively analyzed by Soliz and Fein (1980) and data for corner areas not covered by the Soliz and Fein data set were obtained from National Meteorological Center (NMC) analyses. The time-dependent boundary conditions were generated from observations with a 12 h interval from the initial time to 1200 GMT 14 February. The model covers the area extending from 17.5 to 48.75°N and from 116.25 to 160°E. The horizontal grid size is 1.25° × 1.25° and the time interval of integration is 2 min. Fig. 1 displays the interior of the simulation domain and the sea surface temperatures (SST's) which were used as the lower boundary in this study. The SST's are a 4-day (13–16 February 1975) average obtained from the Navy SST data as achived at the National Center for Atmospheric Research. It is interesting to point out that a warm water tongue stretched from Taiwan to Japan along the

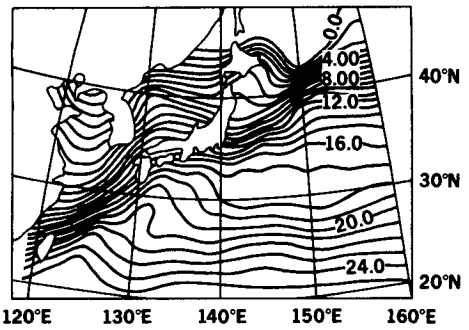

FIG. 1. Sea-surface temperature (°C) used by model. The temperature contour is 1°C.

course of the Kuroshio Current. This warm water area is a favorable place for oceanic cyclogenesis (Nitta and Yamamoto, 1974), much as the Gulf Stream off the east coast of the United States is a favorable area for cyclogenesis. The SST's remained constant during the model integration.

4. Synoptic discussion of the AMTEX cyclone

An overview of the primary features of this cyclone which were used to verify the simulation experiments is presented. For a more complete discussion of this storm see Saito (1977). Fig. 2 depicts the observed

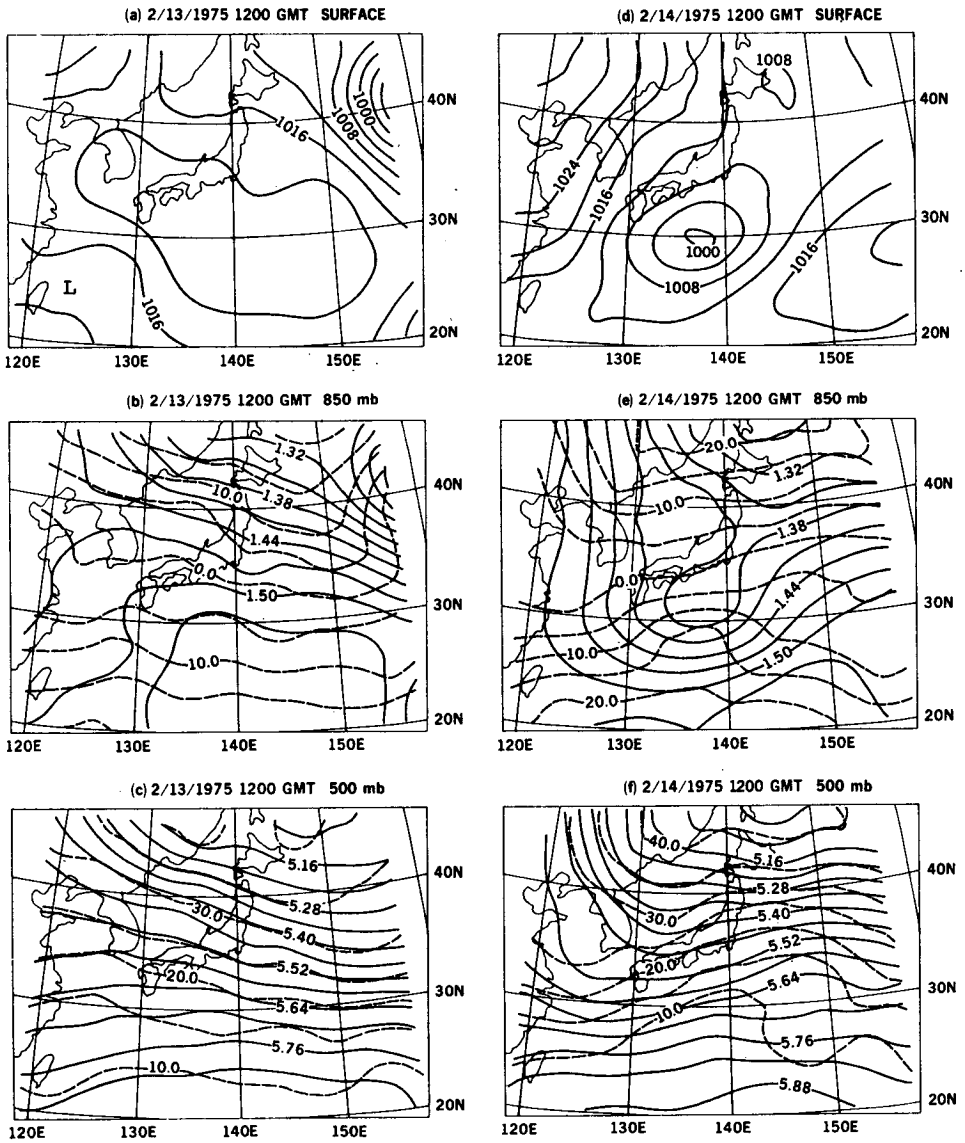

FIG. 2. Observed synoptic conditions for 1200 GMT 13 and 14 February 1975: (a) and (d) are surface pressure with contours every 4 mb; (b) and (e) are 850 mb height (solid lines) and temperature (dashed lines); and (c) and (f) are 500 mb height (solid lines) and temperature (dashed lines). The height contour interval is 0.03 km at 850 mb, and 0.06 km at 500 mb while the temperature interval is 5°C.

surface, 850 and 500 mb synoptic conditions at 1200 GMT 13 and 14 February 1975, the initial and final simulation times. Initially, the computational domain was dominated by high pressure at the surface. A deepening low located at the northeastern corner was moving out of the model domain while a weak surface low-pressure system was located ~150 km east of Taiwan. At 850 mb, a short-wave trough associated with the surface depression supported southerly flow which along with the existing temperature field resulted in warm advection (Saito, 1977). At 500 mb this warm advection was insignificant. Saito (1977, p. 293) describes this system as "warm and confined to below 850 mb." A moist tongue existed above the Kuroshio as evidenced by the precipitable water distribution (not shown). Therefore it was evident that the northward transport of warm moist subtropical maritime air below 850 mb in conjunction with the upward transport of sensible heat and moisture over the Kuroshio was creating potential instability in the lower troposphere. The presence of this instability is depicted by the vertical distribution of moist static energy at 1200 GMT 13 February (dashed lines) in Fig. 3a. The moist static energy was a minimum at ~1 km above the surface. If a lifting source is present, convection is inevitable under these conditions.

During the next 24 h, the surface low-pressure system was transformed into an extratropical oceanic cyclone; at 850 mb the short-wave trough has developed into a warm inverse omega low; and at 500 mb a baroclinic wave with the pressure trough lagging behind the thermal ridge has appeared (Fig. 2). Westward tilting (in the vertical) of the pressure deviation toward cold air, which is characteristic of a developing baroclinic wave, was significant at this stage (Fig. 3b). The upper-level trough, which advected through the simulation's western boundary, and the low-level cyclone have become coupled in the vertical. Also the low-level vertical gradient and the minimum value of the moist static energy at 1 km which existed 24 h before have disappeared, thus indicating that moist convection has neutralized the lower troposphere.

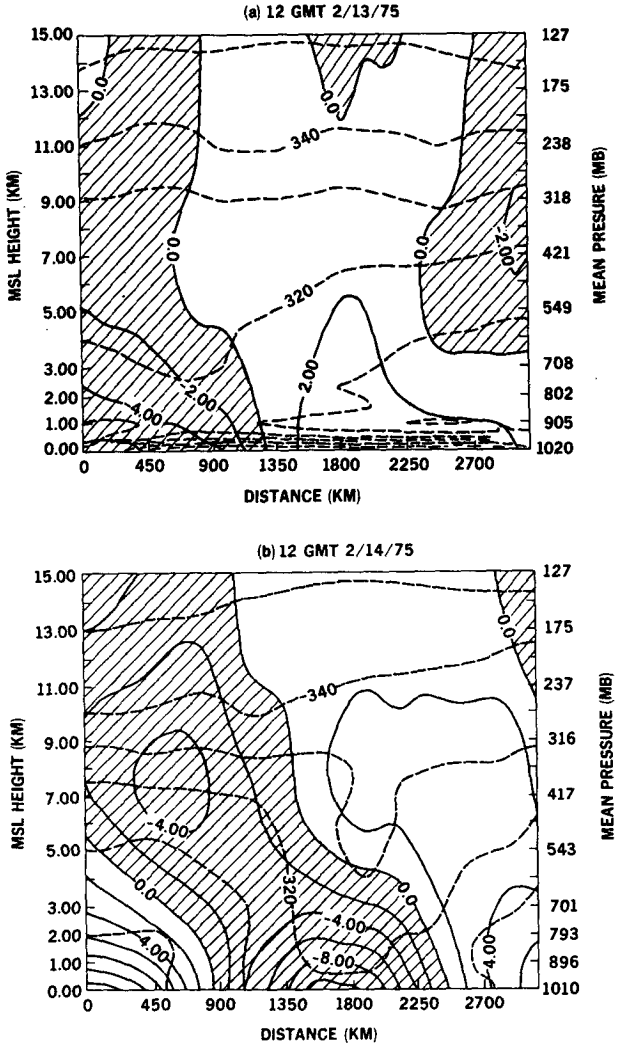

FIG. 3. Cross section of pressure deviation (solid lines) from the west–east mean and moist static energy (dashed lines) along (a) 28°N at 1200 GMT 13 February and (b) 30°N at 1200 GMT 14 February 1975. The pressure contour interval is 2 mb while the moist static energy interval is 10×10^3 m^2 s^{-2}. Negative deviations are shaded for emphasis.

5. Results of the numerical experiments

a. Control experiment

Horizontal maps illustrating the 24 h simulation for the Control are shown in Figs. 4a, 5a and 6a for the surface, 850 and 500 mb, respectively. The most pronounced features of the simulated cyclone at 1200 GMT 14 February were the closed low at the surface south of Japan, the inverse omega low with a warm center at 850 mb, and a thermal ridge east of a pressure trough at 500 mb (compare with Fig. 2). The predicted surface low center was located slightly southwest of the observed system, and its central pressure was ~3 mb higher than the observed value. The simulated surface low was elongated more in the west–east direction while the observed pattern was elongated northeast–southwest.

Although the 850 mb trough of the Control was ~60 m higher than observed, the simulated large-scale flow exhibited an inverse omega low with a warm center similar to that observed. The simulated flow pattern at 500 mb was dominated by a large-scale trough whose trough line tilted (horizontally) northeast–southwest similar to the observations. The simulated trough was not as deep as that observed and the simulated contours east of the trough were more zonally oriented. Consequently, the location of the maximum wind speed (not shown) was displaced somewhat southwestward compared with that observed. This may explain why the simulated surface

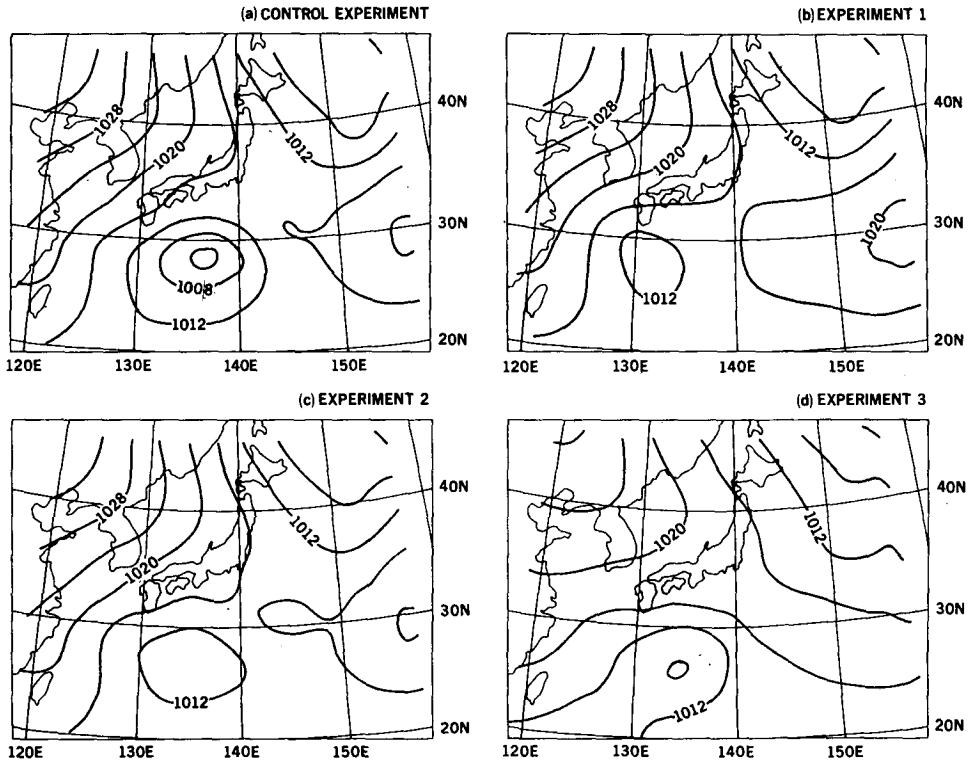

FIG. 4. Simulated 24 h (1200 GMT 14 February) surface pressure for (a) the Control, (b) Experiment 1 (E1), (c) Experiment 2 (E2) and (d) Experiment 3 (E3). The contour interval is 4 mb.

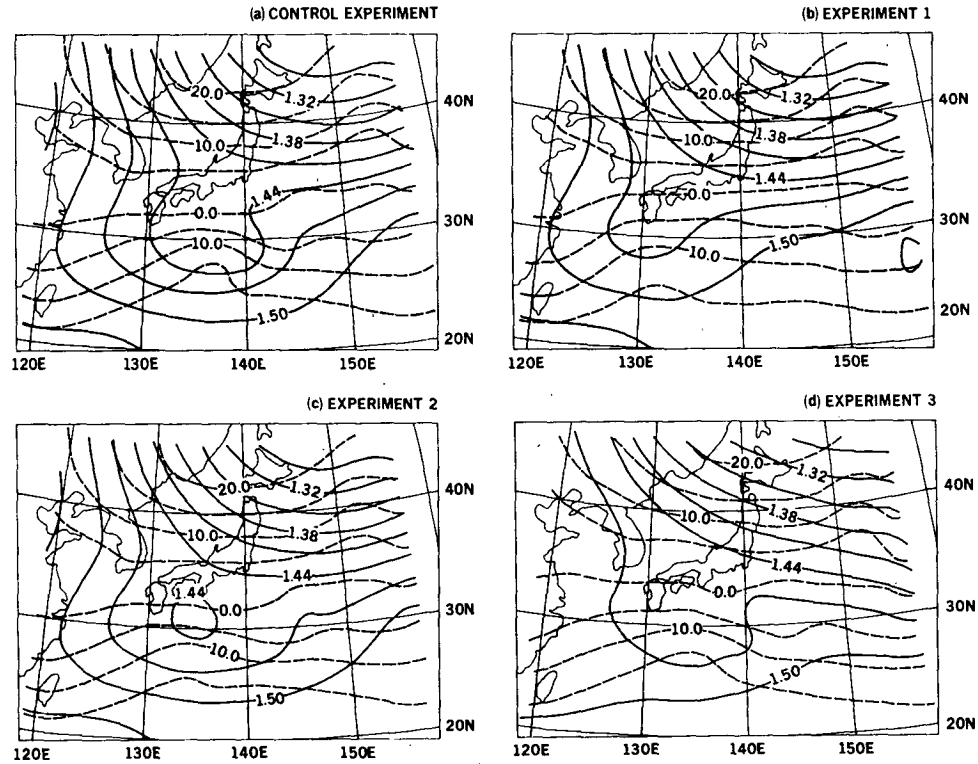

FIG. 5. Simulated 24 h (1200 GMT 14 February) 850 mb height (solid lines) and temperature (dashed lines) for (a) the Control, (b) Experiment 1 (E1), (c) Experiment 2 (E2) and (d) Experiment 3 (E3). The height contour interval is 0.03 km while the temperature interval is 5°C.

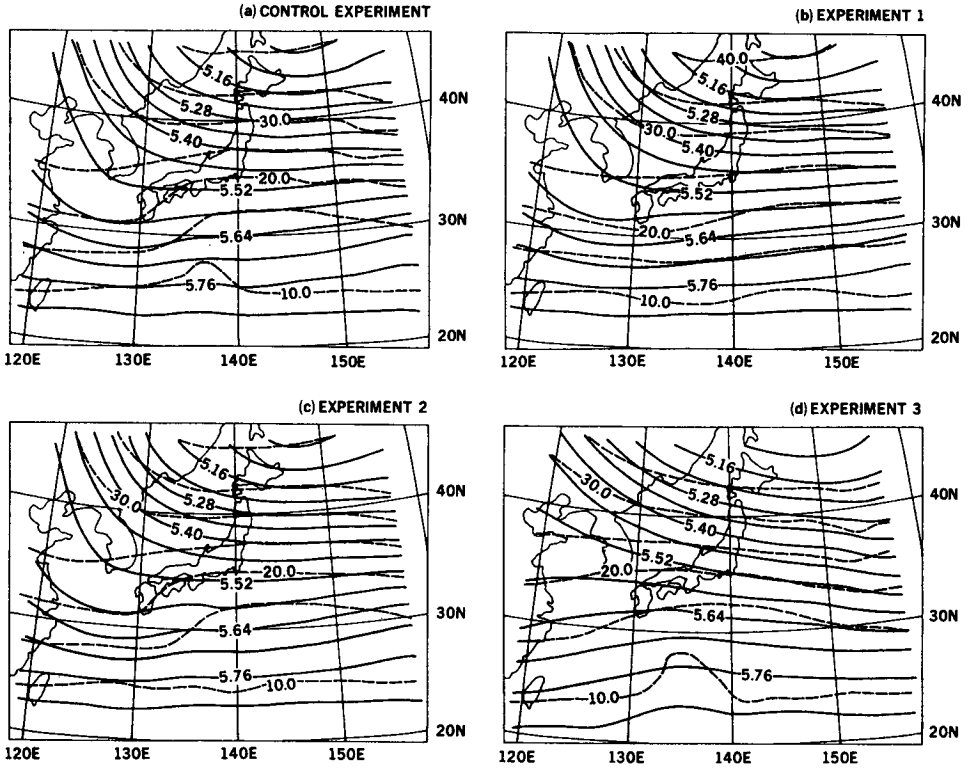

FIG. 6. As in Fig. 5 except at 500 mb and the height interval is 0.06 km.

low center was located slightly southwest of that observed and the simulated surface system was not elongated in the northeast–southwest direction. The simulated synoptic-scale baroclinic wave at 500 mb developed similar to observations.

The 24 h accumulated precipitation predicted by the Control (Fig. 7a; maximum is 51 mm) was distributed in the vicinity of the surface low. Detailed observations of the precipitation at 1200 GMT 14 February over the AMTEX area were not available for a quantitative comparison. However, the AMTEX cyclone cloud structure as analyzed by Thompson *et al.* (1979) (Fig. 8), using satellite infrared radiation data provides indirect information to verify the model performance. As can be seen, the major cloud body was observed to be associated with the surface low. The Thompson *et al.* cloud analysis qualitatively indicates that the simulated precipitation in the Control was reasonable. The Control precipitation is also qualitatively consistent with the diagnostic analysis of the storm's precipitation shown in Wei's (1979) computation of the available potential energy generation.

In view of the discussion above, the 24 h Control simulation has successfully reproduced the major features of this AMTEX cyclone and thus, numerical investigations of the processes involved in the cyclone's development should yield insight into the behavior of the atmosphere as well as the model.

b. Experiments 1, 2 and 3

A brief description of the large-scale features of the E1, E2 and E3 simulations is presented with more detailed comparisons following in Section 6. Again Figs. 4, 5 and 6 illustrate the surface, 850 and 500 mb fields while Fig. 7 depicts the 24 h accumulated precipitation. The central pressure of the simulated surface low in E1–E3 (Fig. 4b–4d) was generally 10 mb higher than that of the observed system. The low center in these experiments were all southwest of that observed, especially E1 which was ~1000 km southwest of that observed. Note that in E3, without lateral boundary forcing, the high pressure center over the eastern part of the domain was missing.

The 850 mb synoptic pattern was characterized by an inverse omega low in all experiments (Figs. 5b–5d). The trough line of each experiment corresponded to 135°E longitude, except for E1 in which the trough line is strongly tilted in the northeast–southwest direction. The main difference between these experiments was in intensity rather than pattern. Furthermore, a warm trough was present in all experiments as indicated by the isotherms.

At 500 mb the height patterns for E1 and E2 (Figs. 6b, 6c) showed a large-scale trough over Japan which did not exist in E3 (Fig. 6d) because the porous sponge boundary condition excluded the eastward movement of the large-scale trough into the model domain.

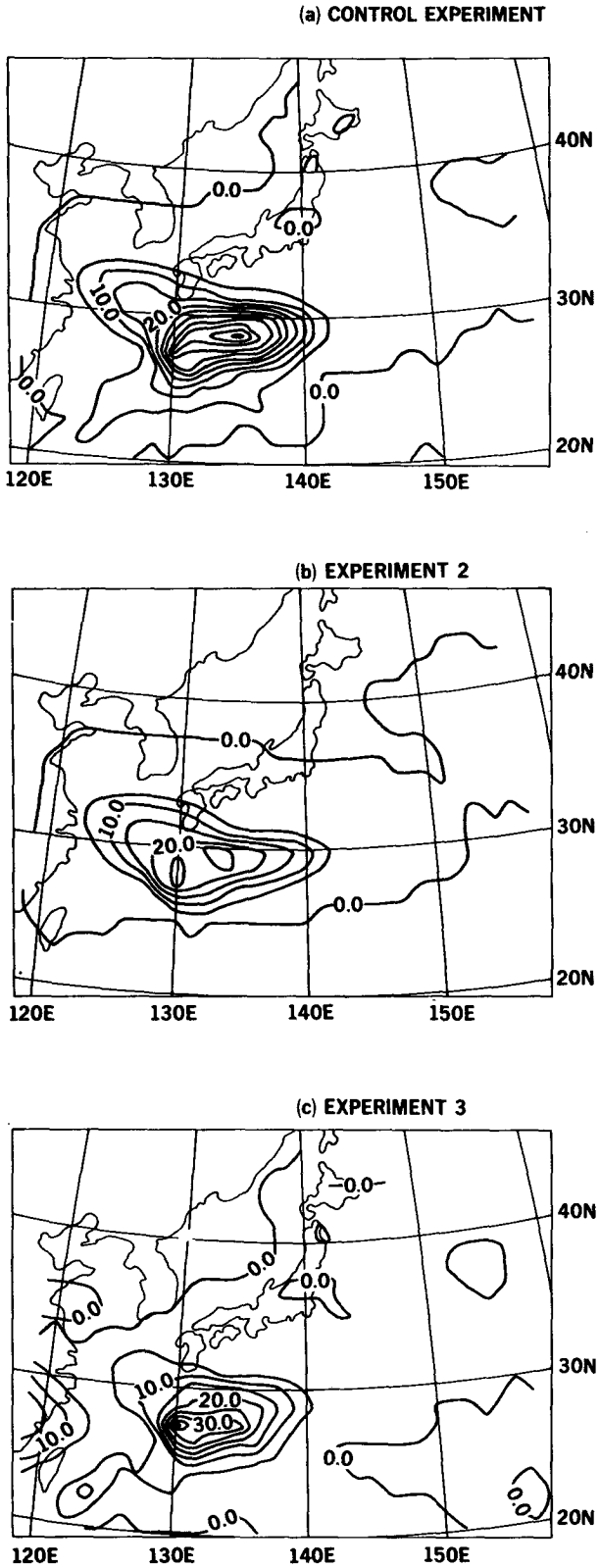

FIG. 7. Simulated 24 h accumulated precipitation for (a) the Control, (b) Experiment 2 (E2) and (c) Experiment 3 (E3). The contour interval is 5 mm.

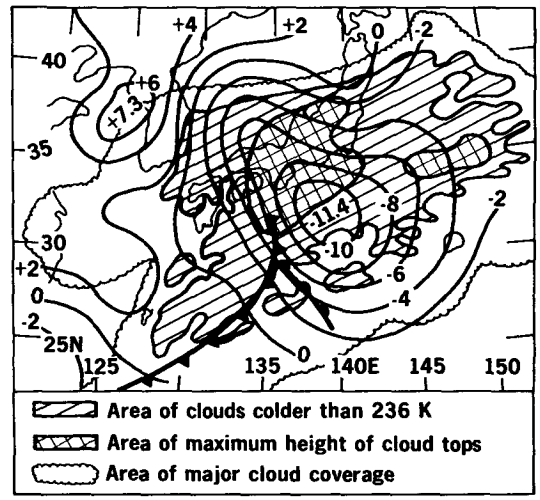

FIG. 8. Analysis of the IR part of the DMSR data for 1200 GMT 14 February 1975. The surface front and the vertical p-velocity (mb h^{-1}) at 700 mb have been added (after Thompson *et al.*, 1979).

In E1 the isotherms were almost parallel to the height contours; in E2 a relatively weak thermal ridge was apparent ahead of the trough.

The 24 h accumulated precipitation for E2 and E3 are shown in Figs. 7b and 7c, respectively (E2 maximum is 27 mm; E3 maximum is 42 mm). Note that the E1 accumulated precipitation was zero. Similar to the Control, the precipitation was closely correlated with the location of the surface low. The maximum accumulation occurred somewhat west of the simulated low center.

6. Comparisons of numerical experiments

As shown in Figs. 4 and 5, the Control produced a deeper surface pressure depression and 850 mb trough in 24 h than E1, E2 or E3. The differences in the central pressure of the surface low and in the geopotential height of the 850 mb trough were on the order of 6 mb and 40 m (~4 mb at 1500 m), respectively. In E3, without large-scale forcing imposed on the lateral boundaries, the pressure gradient associated with the surface high over Asia became relatively weak, and the high over the Pacific disappeared. Although there was not a drastic change in the 850 mb height and temperature patterns due to the changes in model physics, a change in the phase speed of the low-level system was noticeable. It is interesting to note that the impact of the individual physical processes on the model pressure field decreased considerably with height from the surface to 850 mb. Hydrostatically this infers that the largest temperature changes due to changes in physics were at or below 850 mb and only small changes or equal changes with opposite signs were induced in the middle and upper troposphere.

At 500 mb the major differences between the Control and E1, as shown in Fig. 6, were in the temperature fields. In the former case a distinctive thermal ridge developed to the east of the large-scale trough while, in the latter, conditions were more nearly equivalent barotropic. In E2 the baroclinicity associated with the trough was weaker than that in the Control. In E3 the height patterns were almost zonally oriented; nevertheless, a thermal ridge did appear south of Japan. Recall that except for E1 there were moist diabatic processes present in the model. These experiments indicate that the generation of baroclinic conditions in the Control and E2 was primarily attributable to latent heating. This can be further illustrated by the difference maps in 500 mb temperatures shown in Fig. 9. The maximum change (Control minus E1; Fig. 9a) was ~5°C in the area of the thermal ridge. By excluding the heat source at the ocean surface (E2) the amount of total precipitation was reduced by half (Fig. 7b), and hence the intensity of the thermal ridge was also reduced by about half as revealed by the Control minus E2 temperature difference (Fig. 9b). Fig. 10 shows the predicted differences in 300 mb vector wind. Large upper-level

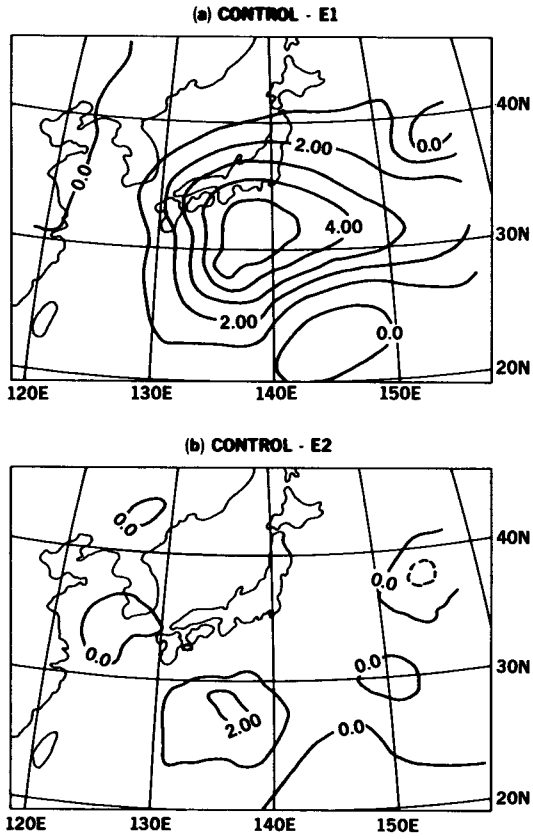

FIG. 9. Simulated 24 h temperature differences at 500 mb for (a) Control minus E1 and (b) Control minus E2. The contour interval is 1°C.

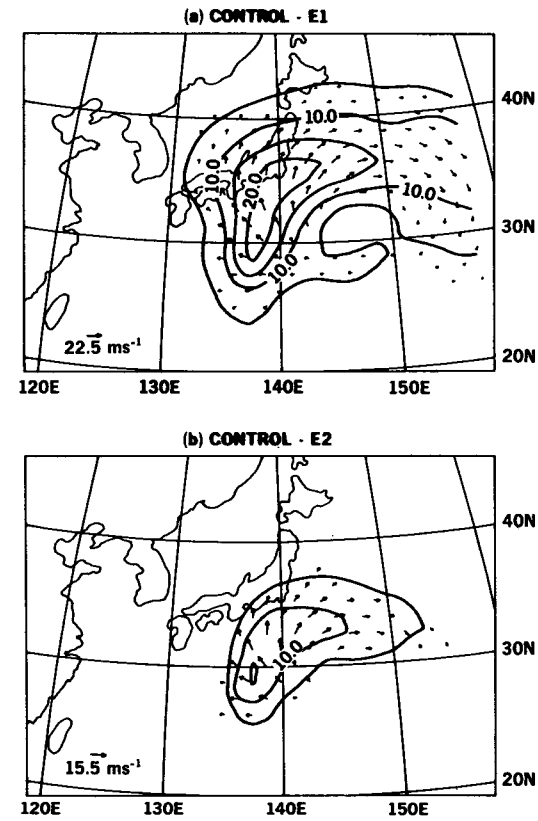

FIG. 10. Simulated 24 h vector wind difference at 300 mb for (a) Control minus E1 and (b) Control minus E2. The speed contour interval is 5 m s^{-1}.

anticyclonic outflow occurred to the northeast of the maximum differences in middle-level temperatures. It is speculated that the generation of negative relative vorticity at these levels may have had a significant impact on the future development of the system.

Figs. 11 and 12 show the simulated 850 mb vorticity and 500 mb vertical motion fields for the Control and the three experiments, respectively. In the control, a large concentration of low-level cyclonic vorticity with strong middle-level ascent existed in the vicinity of the surface cyclone. The relative position between the region of ascent and the cyclone center was in agreement with the observations shown in Fig. 8. The distribution of cyclonic vorticity appeared to be generated by convergence beneath the strong upward motion. The E1 vorticity and vertical motion patterns reflected values more typical of a large-scale circulation than of the observed extratropical storm. Weak downward motion was present to the west of the trough and weak upward motion existed to the east of the trough. There was no indication of the low-level cyclone in the vorticity field. Note that the main change in the dynamic fields from the Control to E1 were in the region of precipitation. In E2 the general vorticity and vertical motion pat-

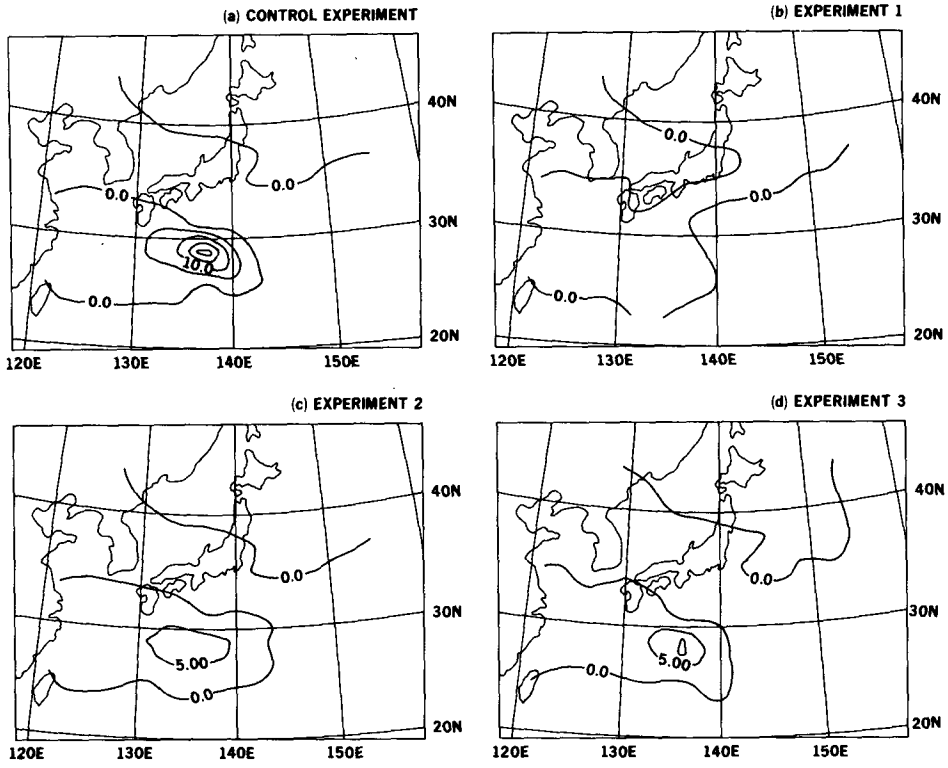

FIG. 11. Simulated 24 h 850 mb relative vorticity for (a) the Control, (b) Experiment 1 (E1), (c) Experiment 2 (E2) and (d) Experiment 3 (E3). The contour interval is 5×10^{-5} s^{-1}.

terns were similar to those of the Control, but the magnitudes were considerably less.

In E3, in spite of much weaker large-scale forcing, the vorticity patterns were similar to those of the Control, but the vertical motion was disorganized. There was no clear organized large-scale feature in the 500 mb vertical motion field as was shown in the other experiments.

As mentioned earlier, the phase speed of the cyclone was affected by the changes in the model physics. This is illustrated by the west–east cross sections of pressure deviation shown in Fig. 13. The region of negative deviation is shaded and the dashed lines represent moist static energy. The Control was similar to the observed profiles (Fig. 3b); for example, note the westward tilt of the pressure trough toward the cold air, the dip of the 320 static energy line into the central portion of the low-level cyclone, and the rather large negative value of pressure deviation below 3 km. The predicted upper-level (7 km and above) pressure deviation was not as strong as observed. This was possibly caused by smoothing of the incoming upper-level trough as it moved into the domain through the western lateral boundary. The Control west–east movement of the surface low was also in essential agreement with the observations.

The eastward speed of the Control's surface cyclone was faster than that of E1 by ~500 km in 24 h. However, the upper-level system was slower in the Control than in E1. An explanation for this paradox is that the latent heat release produced large middle-level warming to the northeast of the surface low center (see Fig. 9). The heating-induced expansion of this air column produced low pressure with cyclonic vorticity generated by convergence near the surface, and high pressure with anticyclonic vorticity generated by divergence aloft (Control versus E1) (see Fig. 10a). This enabled the low-level cyclone to move northeastward while blocking the eastward motion of the upper-level trough. Through these processes the lag between the pressure trough and the thermal ridge, as well as the westward (vertical) tilt, was maintained. Consequently, the cyclogenesis was prolonged and the intensity of the cyclone was enhanced. Without latent heating the upper-level trough quickly moved over the surface depression and the configuration favorable for baroclinic development disappeared.

Both the exclusion of the heat source at the ocean surface (E2) and the lateral boundary forcing (E3) resulted in a reduction of the propagation speed of the surface depression. Recall there was a decrease in precipitation (Fig. 7) and a corresponding decrease in upward vertical motion (Fig. 12) when the heat source was removed. This further emphasizes the significance of the diabatic effects of latent heating on phase speed. Without large-scale lifting the cyclone

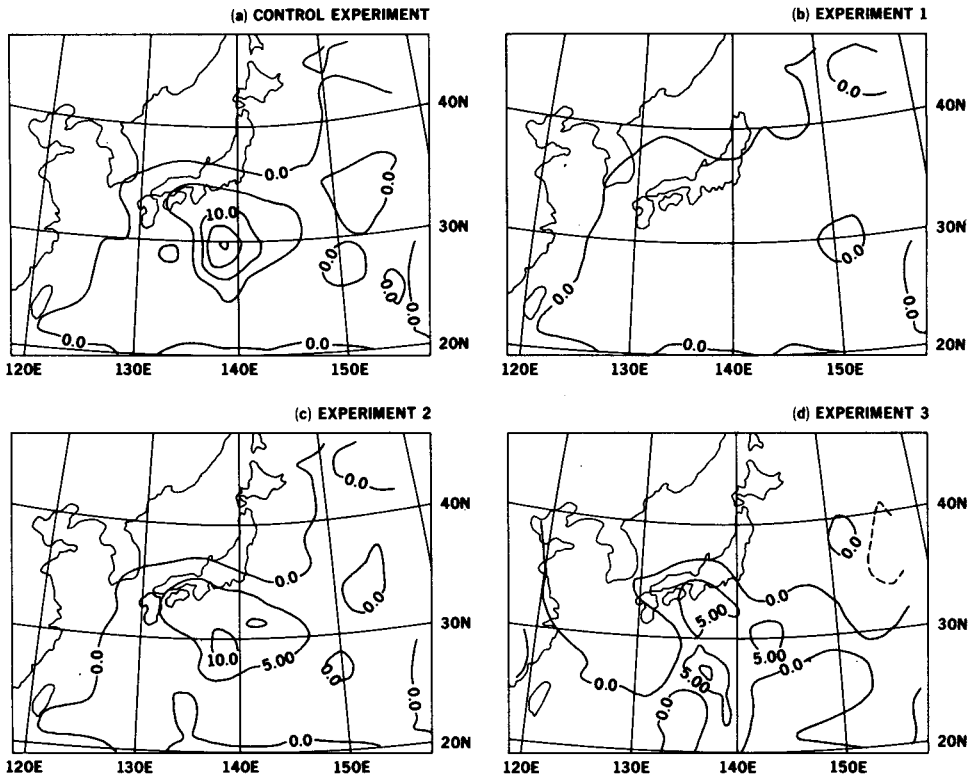

FIG. 12. Simulated 24 h 500 mb vertical velocity for (a) the Control, (b) Experiment 1 (E1), (c) Experiment 2 (E2) and (d) Experiment 3 (E3). The contour interval is 5 cm s^{-1}.

remained very shallow (Fig. 13d). This shallow system was less affected by the upper-level westerlies. Consequently, the cyclone slowed its eastward movement.

7. Summary and concluding remarks

A major winter storm occurred in the initial phase of the 1975 Air Mass Transformation EXperiment (AMTEX). The storm began as a surface low-pressure system which was present at 1200 GMT 13 February 1975 over the ocean east of Taiwan. This weak surface system moved northeastward and developed into an extratropical oceanic cyclone during the next 24 h. A warm inverse omega low developed at 850 mb and a baroclinic wave appeared at 500 mb with a thermal ridge located 1000 km ahead of the height trough.

To determine how latent heat release, sensible heat and moisture fluxes from the ocean, and large-scale forcing affected the evolution of this AMTEX cyclone, a Control and three 24 h numerical experiments were performed using the Drexel Limited-Area Mesoscale Prediction System (LAMPS). The major findings are summarized as follows.

1) The Control experiment (complete physics included) simulated the major features of the AMTEX '75 cyclone faithfully. The capability of the model to generate an intense surface cyclone from a rather weak pressure trough was demonstrated.

2) The latent heat release enhanced the intensification of the oceanic cyclone, the interaction between the upper trough and low-level cyclone, and the middle-level baroclinicity.

3) The prohibition of the sensible heat and moisture fluxes from the sea surface suppressed the moist processes which, in turn, reduced latent heat release and cyclogenesis. The amount of precipitation decreased.

4) The upper-level synoptic-scale had a relatively limited impact on the low-level system in this case. The application of the porous sponge conditions which restricted the eastward propagation of the upper trough did not prevent the formation of the surface cyclone and 850 mb trough; it only weakened them. However, the lack of an upper-level synoptic-scale system did change the overall character of the developing cyclone by decreasing the depth of the system.

5) The phase speed of the low-level cyclone was strongly influenced by latent heating.. Reduction of latent heating resulted in a slower moving cyclone.

These numerical experiments provide quantitative assessment of the physical factors affecting the development of this AMTEX cyclone. Saito (1977) doc-

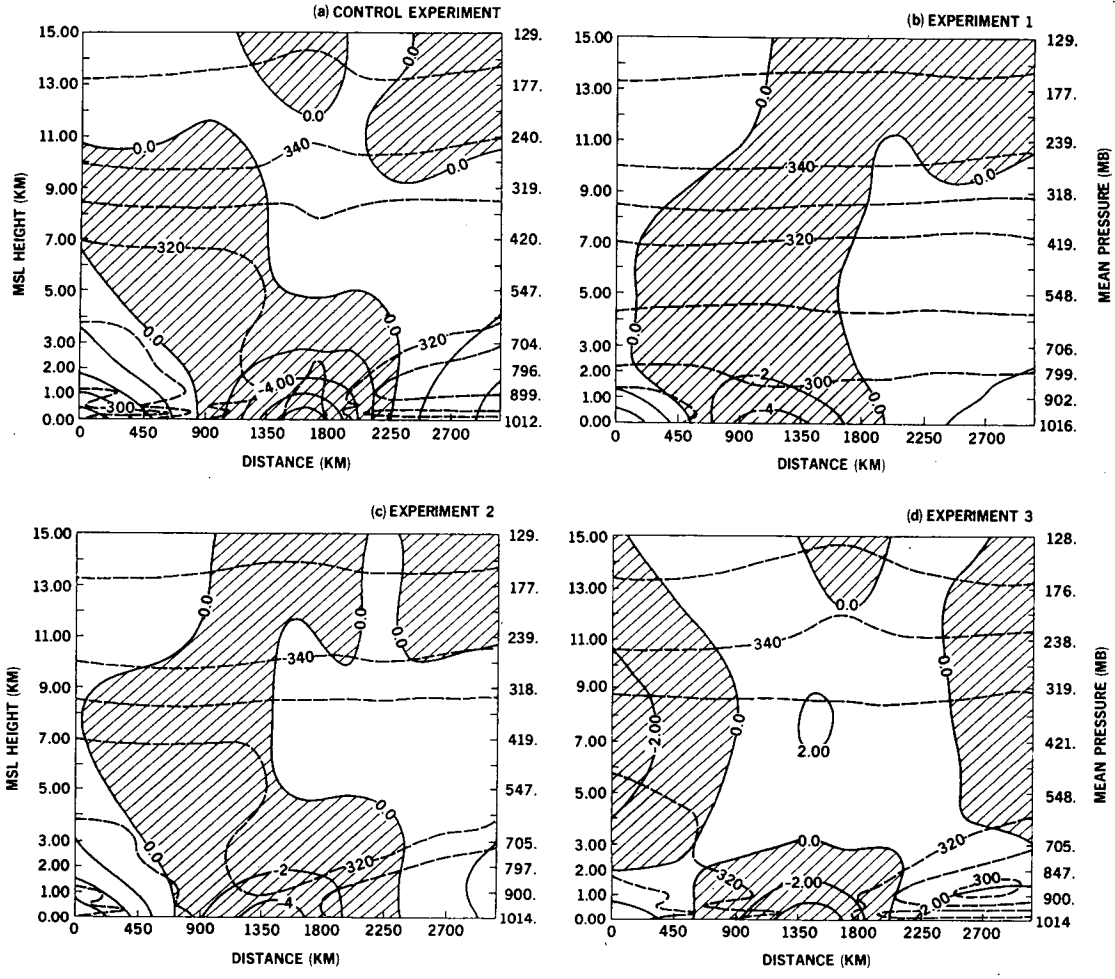

FIG. 13. Simulated 24 h cross section of pressure deviation (solid lines) from the west–east mean and moist static energy (dashed lines). The pressure contour interval is 2 mb while the moist static energy interval is 10×10^3 m^2 s^{-2}. Negative deviations are shaded for emphasis. The cross sections were selected along the latitude through the surface low center of each experiment.

umented that this cyclone was one of three low-level subsynoptic systems during the AMTEX period. In contrast to this system which developed into a synoptic-scale storm, the other two cyclones decayed in less than two days. It would be interesting to numerically examine the evolution of these non-developing cyclones so that a better understanding of oceanic cyclogenesis processes in general could be gained.

Acknowledgments. The data used in this study were provided by the AMTEX group of the University of Oklahoma. We thank Drs. Jay S. Fein, Peter Soliz and Min-Yin Wei for their help in accessing the AMTEX data. Thanks also go to Mr. Gary Glades for producing the computer-drawn graphics and to Mr. Hal G. Marshall for extracting the Navy sea surface temperatures archived at the National Center for Atmospheric Research. Ms. Nadine Perkey helped edit the final draft of this paper. This study was supported by the National Science Foundation under Grant ATM-7951800. The computation and plotting was performed on the CRAY-1 computer at NCAR which is sponsored by the National Science Foundation.

APPENDIX

Governing Equations and Physics of the Drexel LAMPS Model

The prognostic variables are horizontal velocity, virtual potential temperature, specific humidity, cloud water and rain water. The diagnostic variables include the modified Exner function, density and vertical velocity. The modified Exner function is defined as

$$\pi = c_p(P/1000)^{R/c_p}.$$

The equations and physics of the LAMPS model summarized from the description by Kreitzberg (1978) and Chang *et al.* (1981) are as follows:

a. Basic governing equations:

1) Conservation of momentum
2) Conservation of energy
3) Conservation of moisture
4) Hydrostatic equation
5) Mass continuity equation
6) Equation of state.

b. Physics:

1) Stable heating due to grid-scale condensation and evaporation
2) Parameterization of subgrid-scale moist and dry convection by the sequential plume model described by Kreitzberg and Perkey (1976, 1977)
3) Parameterization of the surface and planetary boundary layers with a simple surface energy balance (Gadd and Keers, 1970) for estimating the surface heat and moisture flux
4) Horizontal and vertical diffusion.

The major numerical aspects of the model discussed by Perkey (1976) are as follows:

1) An unstaggered grid with all quantities defined at all grid points
2) Second-order central time differencing with weak time filtering
3) Fourth-order central spatial differencing in the horizontal
4) Second-order central spatial differencing in the vertical
5) $d/dt = 0$ at the model top
6) Either the porous sponge conditions or time-dependent lateral boundary conditions (Perkey and Kreitzberg, 1976).

REFERENCES

Agee, E. M., and R. P. Howley, 1977: Latent and sensible heat flux calculations at the air–sea interface during AMTEX 74. *J. Appl. Meteor.*, **16,** 443–447.

Chang, C.-B., D. J. Perkey and C. W. Kreitzberg, 1981: A numerical case study of the squall line of 6 May 1975. *J. Atmos. Sci.*, **38,** 1601–1615.

Chen, T.-C., and C.-B. Chang, 1982: Synoptic study of an ocean cyclone during AMTEX 75. Tech. Rep. ATM-7951800, to National Science Foundation Meteor. Prog., Dept. Earth Sci., Iowa State University, 37 pp.

Gadd, A., and J. F. Keers, 1970: Surface exchange of sensible and latent heat in a 10-level model atmosphere. *Quart. J. Roy. Meteor. Soc.*, **96,** 297–306.

Joint Scientific Committee for GARP, 1981: *Scientific Results of the Air Mass Transformation Experiment (AMTEX).* GARP Pub. Ser., No. 24, 236 pp.

Kreitzberg, C. W., 1978: Progress and problems in regional numerical weather prediction. *Proc. SIAM,* **11,** Amer. Math. Soc., 32–58.

——, and D. J. Perkey, 1976: Release of potential instability. Part I: A sequential plume model within a hydrostatic primitive equation model. *J. Atmos. Sci.*, **33,** 456–475.

——, and ——, 1977: Release of potential instability. Part II: The mechanism of convective/mesoscale interaction. *J. Atmos. Sci.*, **34,** 1569–1595.

Kung, E. C., and A. J. Siegel, 1979: A study of heat and moisture budgets in the intense winter monsoon over the warm ocean current. *J. Atmos. Sci.*, **36,** 1880–1894.

Nitta, T., and J.-I. Yamamoto, 1974: On the observational characteristics of intermediate scale disturbances generated near Japan and the vicinity. *J. Meteor. Soc. Japan,* **52,** 11–30.

Perkey, D. J., 1976: A description and preliminary results from a fine-mesh model for forecasting quantitative precipitation. *Mon. Wea. Rev.*, **104,** 1513–1526.

——, and C. W. Kreitzberg, 1976: A time-dependent lateral boundary scheme for limited-area primitive equation models. *Mon. Wea. Rev.*, **104,** 744–755.

Saito, N., 1977: On the structure of a medium-scale depression over the East China Sea during AMTEX '75. *J. Meteor. Soc. Japan,* **55,** 286–300.

Sheu, P. J., and E. M. Agee, 1977: Kinematic analysis and air-sea heat flux associated with mesoscale cellular convection during AMTEX 75. *J. Atmos. Sci.*, **34,** 793–801.

Soliz, P., and J. S. Fein, 1980: Kinematic analysis for a major winter storm during AMTEX '75. *J. Meteor. Soc. Japan,* **58,** 16–32.

Thompson, A. H., W. K. Henry, J. R. Mills and A. R. Laing, 1979: Cloud structure with a developing "Taiwan Low" as indicated by satellite infrared radiation data. *Pap. Meteor. Res.*, **2,** 75–86.

Wei, M.-Y., 1979: The energy budgets of a developing cyclone over the East China Sea during the 1975 Air Mass Transformation Experiment. Ph.D. dissertation, University of Oklahoma, Norman, 136 pp.